

# LOWER EIGENVALUE BOUNDS WITH HYBRID HIGH-ORDER METHODS

NGOC TIEN TRAN

**ABSTRACT.** This paper proposes hybrid high-order eigensolvers for the computation of guaranteed lower eigenvalue bounds. These bounds display higher order convergence rates and are accessible to adaptive mesh-refining algorithms. The involved constants arise from local embeddings and are available for all polynomial degrees. Applications include the linear elasticity and Steklov eigenvalue problem.

## 1. INTRODUCTION

**1.1. Motivation.** Guaranteed error control for the approximation of eigenvalues associated with positive definite partial differential equations requires upper and lower bounds of the exact eigenvalue  $\lambda(j)$ . While upper bounds can be achieved by conforming methods using the Rayleigh-Ritz principle, lower bounds are more challenging to obtain. The first lower eigenvalue bounds (LEB) are computed in [22, 6] and the ideas therein have been extended to other problems [5, 24, 21] as well. Recently, mixed methods [20] provide LEB for a large range of examples with an additional benefit. The involved constants are independent of the explicit discretization. The bounds of all aforementioned methods are postprocessings of the computed eigenvalue  $\lambda_h(j)$  of the form

$$\frac{\lambda_h(j)}{1 + \delta \lambda_h(j)} \leq \lambda(j).$$

They are restricted to lowest-order convergence because, in practice, the parameter  $\delta$  has a fixed scaling in terms of maximal mesh-size arising from some local compact embeddings. Thus, higher-order methods cannot provide any improvement and uniform mesh-refining algorithms may even outperform adaptive computations in certain examples on nonconvex domains [9].

A remedy is [11] with a hybrid high-order (HHO) eigensolver [16, 15] plus the Lehrenfeld-Schörberl stabilization, where the computed eigenvalue  $\lambda_h(j) \leq \lambda(j)$  is a direct LEB of  $\lambda$  under an explicit assumption on the maximal mesh-size. This makes the bound accessible to higher-order discretizations and adaptivity. Other HHO schemes for the Laplace eigenvalue problem has been considered in [4, 7] with optimal convergence rates of adaptive mesh-refining algorithms in [8] for the lowest-order case. The limitation of all aforementioned contributions is the restriction to the Laplace eigenvalue problem and the involved constants are *only* guaranteed for lowest-order discretizations.

---

*Date:* 11th June 2024.

*2020 Mathematics Subject Classification.* 65N25, 65N30.

*Key words and phrases.* lower eigenvalue bounds, hybrid high-order.

This project received funding from the European Union's Horizon 2020 research and innovation programme (project RandomMultiScales, grant agreement No. 865751).

In this paper, we propose four abstract conditions based on the observations of [11] that imply the LEB bound

$$(1.1) \quad \text{LEB}(j) := \min\{1, 1/(\alpha + \beta\lambda_h(j))\}\lambda_h(j) \leq \lambda(j)$$

with the convention  $\text{LEB}(j) := 0$  for  $\lambda_h(j) = \infty$ . In practice,  $\alpha < 1$  is a chosen parameter and  $\beta$  is an explicit constant with a positive scaling of the maximal mesh-size. Therefore,  $\lambda_h(j) \leq \lambda(j)$  eventually holds whenever  $\alpha + \beta\lambda_h(j) < 1$ . The main contribution is the design of HHO methods that allow for guaranteed constants independent of the polynomial degree. As an extra benefit, hanging nodes are allowed as long as mesh is partitioned into convex cells for additional flexibility in the mesh design. Since the presented approach relies on intrinsic features of the HHO methodology, it applies to a wide range of examples including linear elasticity and Steklov eigenvalue problems.

**1.2. Setting.** Given a Hilbert space  $V$ , the eigenvalue problem of this paper seeks eigenvalues  $\lambda$  and eigenvectors  $u \in V$  such that

$$(1.2) \quad a(u, v) = \lambda b(u, v) \quad \text{for any } v \in V.$$

with a scalar product  $a$  in  $V$  and a symmetric positive semidefinite bilinear form  $b : V \times V \rightarrow \mathbb{R}$ . They induce the norm  $\|\bullet\|_a$  and the seminorm  $\|\bullet\|_b$  in  $V$ . We assume the following setting. The finite eigenvalues  $0 < \lambda(1) \leq \lambda(2) \leq \dots < \infty$  are given by the Rayleigh-Ritz principle

$$(1.3) \quad \lambda(j) = \min_{W \subset V, \dim(W)=j} \max_{v \in W \setminus \{0\}} \|v\|_a^2 / \|v\|_b^2.$$

The eigenvectors  $u(1), u(2), \dots$  are subject to the normalization  $\|u(j)\|_b = 1$  and satisfy the orthogonality

$$(1.4) \quad a(u(j), u(k)) = b(u(j), u(k)) = 0 \quad \text{for any } j \neq k.$$

Let  $V_{\text{nc}}$  be some piecewise version of  $V \subset V_{\text{nc}}$  with respect to a mesh, endowed with the seminorm  $\|\bullet\|_{a_{\text{pw}}}$  induced by a positive semidefinite bilinear form  $a_{\text{pw}}$  in  $V_{\text{nc}}$ . It is not required that  $a_{\text{pw}}$  is an extension of  $a$  to  $V_{\text{nc}}$ . On the discrete level,  $V_h$  denotes the discrete ansatz space with an interpolation  $I_h : V \rightarrow V_h$ . The prototypical HHO eigensolver seeks eigenvalues  $\lambda_h$  and eigenvectors  $u_h$  such that

$$(1.5) \quad a_h(u_h, v_h) + s_h(u_h, v_h) = \lambda_h b_h(u_h, v_h)$$

with symmetric positive semidefinite bilinear forms  $a_h, b_h, s_h : V_h \times V_h \rightarrow \mathbb{R}$ , which define the seminorms  $\|\bullet\|_{a_h}$ ,  $\|\bullet\|_{b_h}$ , and  $\|\bullet\|_{s_h}$ . In the HHO methodology,  $s_h$  is called stabilization and  $a_h + s_h$  on the left-hand side of (1.5) is a scalar product in  $V_h$ . Similar to the continuous level, the discrete eigenvalues  $0 \leq \lambda_h(1) \leq \dots \leq \lambda_h(N) \leq \infty$  with  $N := \dim V_h$  satisfy the Rayleigh-Ritz principle

$$(1.6) \quad \lambda_h(j) = \min_{W_h \subset V_h, \dim(W_h)=j} \max_{v_h \in W_h \setminus \{0\}} (\|v_h\|_{a_h}^2 + \|v_h\|_{s_h}^2) / \|v_h\|_{b_h}^2.$$

**1.3. Framework.** For the sake of brevity, we consider the Dirichlet eigenvalue problem in this introduction with  $V = H_0^1(\Omega)$ ,  $a := (\nabla \bullet, \nabla \bullet)_{L^2(\Omega)}$ ,  $b := (\bullet, \bullet)_{L^2(\Omega)}$ ,  $V_{\text{nc}} := H^1(\mathcal{M})$  for a mesh  $\mathcal{M}$  into convex polyhedra, and  $a_{\text{pw}} := (\nabla_{\text{pw}} \bullet, \nabla_{\text{pw}} \bullet)_{L^2(\Omega)}$ . The ansatz space  $V_h := P_{k+1}(\mathcal{M}) \times P_k(\Sigma(\Omega))$  consists of piecewise polynomials on  $\mathcal{M}$  and  $\Sigma(\Omega)$ , the set of all interior sides, with the interpolation  $I_h v := (\Pi_{\mathcal{M}}^{k+1} v, \Pi_{\Sigma}^k v) \in V_h$  for  $v \in V$ . Here,  $\Pi_{\mathcal{M}}^{k+1}$  and  $\Pi_{\Sigma}^k$  denote the  $L^2$  projection onto the discrete spaces  $P_{k+1}(\mathcal{M})$  and  $P_k(\Sigma(\Omega))$ . The piecewise gradient of a potential reconstruction  $\mathcal{R}_h : V_h \rightarrow W_{\text{nc}}$  in the discrete subspace  $W_{\text{nc}} := P_{k+1}(\mathcal{M})$  of  $V_{\text{nc}}$  approximates the differential operator  $\nabla$ . This defines  $a_h := a_{\text{pw}}(\mathcal{R}_h \bullet, \mathcal{R}_h \bullet)$  and  $b_h(u_h, v_h) := (u_{\mathcal{M}}, v_{\mathcal{M}})_{L^2(\Omega)}$  for any  $u_h = (u_{\mathcal{M}}, u_{\Sigma})$ ,  $v_h = (v_{\mathcal{M}}, v_{\Sigma}) \in V_h$ . Further

details on the discretization follow in Section 3 below. A characteristic feature is the connection

$$(1.7) \quad \mathcal{R}_h \circ \mathbf{I}_h = \mathbf{G}_h \quad \text{in } V$$

between  $\mathcal{R}_h$  and a Galerkin projection  $\mathbf{G}_h : V_{\text{nc}} \rightarrow W_{\text{nc}}$ , defined, for given  $v \in V_{\text{nc}}$ , as a solution to

$$(1.8) \quad a_{\text{pw}}(\mathbf{G}_h v, \varphi_{\text{nc}}) = a_{\text{pw}}(v, \varphi_{\text{nc}}) \quad \text{for any } \varphi_{\text{nc}} \in W_{\text{nc}}.$$

Notice that  $a_{\text{pw}}$  may not be a scalar product in  $W_{\text{nc}}$  in general and therefore, the unique definition of  $\mathbf{G}_h$  additionally requires fixing the degrees of freedom associated with the kernel of  $a_{\text{pw}}$ , e.g.,

$$(1.9) \quad \int_K \mathbf{G}_h v \, dx = \int_K v \, dx \quad \text{for any } K \in \mathcal{M}$$

in the present model problem. From (1.8), we infer the orthogonality  $v - \mathbf{G}_h v \perp_{a_{\text{pw}}} W_{\text{nc}}$ . Together with (1.7), this shows, for any  $v \in V$ , that

$$(A) \text{ (} a\text{-orthogonality) } \|\mathbf{I}_h v\|_{a_h}^2 \leq \|v\|_a^2 - \|v - \mathbf{G}_h v\|_{a_{\text{pw}}}^2$$

(even with equality for this example). In particular,

$$(1.10) \quad \|v - \mathbf{G}_h v\|_{a_{\text{pw}}}^2 \leq \|v\|_a^2.$$

The quasi-best approximation property

$$(B) \text{ (scaling of stabilization) } \|\mathbf{I}_h v\|_{s_h}^2 \leq \alpha \|v - \mathbf{G}_h v\|_{a_{\text{pw}}}^2$$

of the stabilization with a positive constant  $\alpha$  is utilized in many contributions [18, 2, 10]. The proposed stabilization in this paper allows for some  $\alpha$  independent of the polynomial degree  $k$ . The final ingredient towards LEB involves the compact embedding  $\|v - \mathbf{G}_h v\|_{L^2(\Omega)}^2 \leq \beta \|v - \mathbf{G}_h v\|_{a_{\text{pw}}}^2$  with  $\beta \leq h_{\text{max}}^2/\pi^2$  from a Poincaré inequality [1]. This, the Pythagoras theorem  $\|\mathbf{I}_h v\|_{b_h}^2 = \|v\|_b^2 - \|v - \Pi_{\mathcal{M}}^{k+1} v\|_{L^2(\Omega)}^2$ , and  $\|v - \Pi_{\mathcal{M}}^{k+1} v\|_{L^2(\Omega)} \leq \|v - \mathbf{G}_h v\|_{L^2(\Omega)}$  allow for

$$(C) \text{ (} b\text{-orthogonality) } \|\mathbf{I}_h v\|_{b_h}^2 \geq \|v\|_b^2 - \beta \|v - \mathbf{G}_h v\|_{a_{\text{pw}}}^2.$$

Utilising similar arguments to [11], we deduce from (A)–(C) the LEB (1.1). Since (A)–(C) are not restricted to the Dirichlet eigenvalue problem, the results of this paper are applicable to other examples as well.

**1.4. Outline.** The remaining parts of this paper are organized as follows. Section 2 establishes (1.1) from (A)–(C). The remaining sections apply the results from Section 2 to the Laplacian (Section 3), Steklov eigenvalue problem (Section 4), linear elasticity (Section 5), and computation of constants in compact embeddings (Section 6).

**1.5. Notation.** Standard notation for Lebesgue and Sobolev spaces applies throughout this paper with the abbreviations  $(\varphi, \psi)_{L^2(\Omega)}$  for the  $L^2$  scalar product of two functions  $\varphi, \psi \in L^2(\Omega)$ .

## 2. LOWER EIGENVALUE BOUNDS

In the setting of Subsection 1.2, we recall the results from the introduction.

**Theorem 2.1 (LEB).** *Suppose that there exists an operator  $\mathbf{G}_h : V_{\text{nc}} \rightarrow W_{\text{nc}}$  onto a discrete subspace  $W_{\text{nc}} \subset V_{\text{nc}}$  of  $V_{\text{nc}}$  and positive constants  $\alpha, \beta > 0$  with (A)–(C) for any  $v \in V$ . Then (1.1) holds for any  $j = 1, \dots, N$ .*

The proof of Theorem 2.1 utilizes the following observation. Define the finite dimensional subspace  $W := \text{span}\{u(1), \dots, u(j)\}$  of  $V$ .

**Lemma 2.2** (linear independency). *If  $\beta\lambda(j) < 1$ , then (a)–(b) hold.*

- (a) *The interpolations  $I_h u(1), \dots, I_h u(j)$  of the exact eigenvectors  $u(1), \dots, u(j)$  are linearly independent in  $V_h$ .*  
 (b) *Suppose additionally  $\lambda_h < \infty$ , then there exists  $v \in W$  with  $\|v\|_b = 1$  and*

$$(1 - \alpha - \beta\lambda_h(j))\|v - G_h v\|_{a_{pw}}^2 \leq \lambda(j) - \lambda_h(j).$$

*Proof.* The proof of Lemma 2.2 follows the arguments of [11] and is outlined below for the sake of completeness.

*Proof of (a).* Suppose otherwise, then there are real numbers  $t_1, \dots, t_n$  such that  $v := t_1 u(1) + \dots + t_j u(j)$  satisfies  $\|v\|_b = 1$  but  $I_h v = 0$ . (The normalization  $\|v\|_b = 1$  is possible because  $b$  is a norm in  $\text{span}\{u(1), \dots, u(j)\}$ .) The orthogonality in (1.4) proves  $1 = \|v\|_b^2 = t_1^2 \|u(1)\|_b^2 + \dots + t_j^2 \|u(j)\|_b^2 = t_1^2 + \dots + t_j^2$ . Elementary algebra with (1.4) yields

$$\begin{aligned} \|v\|_a^2 &= t_1^2 \|u(1)\|_a^2 + \dots + t_j^2 \|u(j)\|_a^2 = t_1^2 \lambda(1) + \dots + t_j^2 \lambda(j) \\ (2.1) \quad &\leq (t_1^2 + \dots + t_j^2) \lambda(j) = \lambda(j). \end{aligned}$$

The combination of this with (C) and (1.10) results in

$$(2.2) \quad 1 = \|v\|_b^2 \leq \beta \|v - G_h v\|_{a_{pw}}^2 \leq \beta \|v\|_a^2 \leq \beta \lambda(j);$$

a contradiction to  $\beta\lambda(j) < 1$ .

*Proof of (b).* Since the interpolations  $I_h u(1), \dots, I_h u(j)$  are linearly independent from (a),  $I_h W \subset V_h$  is a  $j$ -dimensional subspace of  $V_h$ . The Rayleigh-Ritz principle (1.6) on the discrete level shows

$$\lambda_h(j) \leq \max_{v_h \in I_h W \setminus \{0\}} (\|v_h\|_{a_h}^2 + \|v_h\|_{s_h}^2) / \|v_h\|_{b_h}^2.$$

Let  $v \in W \setminus \{0\}$  with  $\|v\|_b = 1$  be given such that  $I_h v$  is a maximizer of this Rayleigh quotient (which can attain the value  $+\infty$ ). Then

$$(2.3) \quad \lambda_h(j) \|I_h v\|_{b_h}^2 \leq \|I_h v\|_{a_h}^2 + \|I_h v\|_{s_h}^2.$$

From (A) and  $\|v\|_a^2 \leq \lambda(j)$  in (2.1), we deduce that  $\|I_h v\|_{a_h}^2 \leq \lambda(j) - \|v - G_h v\|_{a_{pw}}^2$ . This and (B) imply that the right-hand side of (2.3) is bounded by  $\lambda(j) - (1 - \alpha) \|v - G_h v\|_{a_{pw}}^2$ , while  $\lambda_h(j)(1 - \beta \|v - G_h v\|_{a_{pw}}^2)$  is a lower bound for the left-hand side of (2.3) thanks to (C) and  $\|v\|_b = 1$ . Hence,

$$\lambda_h(j)(1 - \beta \|v - G_h v\|_{a_{pw}}^2) \leq \lambda(j) - (1 - \alpha) \|v - G_h v\|_{a_{pw}}^2.$$

Reorganizing these terms concludes the proof of (b).  $\square$

*Proof of Theorem 2.1.* Fix  $1 \leq j \leq N$ . Recall the convention  $\text{LEB}(j) := 0$  for  $\lambda_h(j) = \infty$ , which is a trivial bound for  $\lambda(j)$ . Hence, throughout this proof, we assume that  $\lambda_h < \infty$ . The proof consists of two cases (a)  $\alpha + \beta\lambda_h(j) \leq 1$  and (b)  $\alpha + \beta\lambda_h(j) > 1$ .

(a) Suppose that  $\alpha + \beta\lambda_h(j) \leq 1$ , then the assertion reads  $\lambda_h(j) \leq \lambda(j)$ . If  $\beta\lambda(j) \geq 1$ , then  $\beta\lambda_h(j) \leq \alpha + \beta\lambda_h(j) \leq 1 \leq \beta\lambda(j)$ , whence  $\lambda_h(j) \leq \lambda(j)$ . If  $\beta\lambda(j) < 1$ , then Lemma 2.2(b) and  $1 - \alpha - \beta\lambda_h(j) \geq 0$  imply  $\lambda_h(j) \leq \lambda(j)$ .

(b) Suppose that  $\alpha + \beta\lambda_h(j) > 1$ , then the claim reads  $\lambda_h(j)/(\alpha + \beta\lambda_h(j)) \leq \lambda(j)$ . If  $\beta\lambda(j) < 1$ , then Lemma 2.2(b) implies the existence of a  $v \in W$  with  $\|v\|_b = 1$  and  $(1 - \alpha - \beta\lambda_h(j))\|v - G_h v\|_{a_{pw}}^2 \leq \lambda(j) - \lambda_h(j)$ . The normalization  $\|v\|_b = 1$  implies  $\|v\|_a^2 \leq \lambda(j)$  and so,  $\|v - G_h v\|_{a_{pw}}^2 \leq \|v\|_a^2 \leq \lambda(j)$  from (1.10). This,  $1 - \alpha - \beta\lambda_h(j) < 0$ , and  $(1 - \alpha - \beta\lambda_h(j))\|v - G_h v\|_{a_{pw}}^2 \leq \lambda(j) - \lambda_h(j)$  provide

$$(1 - \alpha - \beta\lambda_h(j))\lambda(j) \leq \lambda(j) - \lambda_h(j),$$

whence  $\lambda_h(j)/(\alpha + \beta\lambda_h(j)) \leq \lambda(j)$ . If  $1 \leq \beta\lambda(j)$ , then  $\lambda_h(j)/(\alpha + \beta\lambda_h(j)) \leq 1/\beta \leq \lambda(j)$ . This concludes the proof.  $\square$

As in [11, 4, 2], the conditions (A)–(C) allow for LEB from a priori information on the exact eigenvalue.

**Corollary 2.3** (a priori LEB). *If  $\alpha + \beta\lambda(j) \leq 1$  and  $\lambda_h(j) < \infty$ , then  $\lambda_h(j) \leq \lambda(j)$ .*

*Proof.* The bounds  $\alpha + \beta\lambda(j) \leq 1$  implies  $1 - \alpha - \beta\lambda_h(j) \geq \alpha + \beta\lambda(j) - \alpha - \beta\lambda_h(j) \geq \beta(\lambda(j) - \lambda_h(j))$ . Since  $\beta\lambda(j) < 1$ , Lemma 2.2(b) holds and therefore,

$$(2.4) \quad \beta(\lambda(j) - \lambda_h(j))\|v - G_h v\|_{a_{pw}}^2 \leq \lambda(j) - \lambda_h(j)$$

for some  $v \in V$  with  $\|v\|_b = 1$ . Recall  $\beta\|v - G_h v\|_{a_{pw}}^2 \leq \beta\|v\|_a^2 \leq \beta\lambda(j)$  From (1.10) and (2.1). This and (2.4) provide

$$\beta\lambda(j)(\lambda(j) - \lambda_h(j)) \leq \lambda(j) - \lambda_h(j).$$

This inequality can only hold if  $\lambda_h(j) \leq \lambda(j)$  because  $\beta\lambda(j) < 1$ .  $\square$

### 3. LAPLACE OPERATOR

The remaining parts of this paper are devoted to the application of Theorem 2.1 to different model problems. Let  $\Omega \subset \mathbb{R}^n$  be an open bounded polyhedral Lipschitz domain in two or three space dimensions  $n = 2, 3$ . The first example seeks eigenpairs  $(\lambda, u)$  with

$$(3.1) \quad -\Delta u = \lambda u \text{ in } \Omega \quad \text{and} \quad u = 0 \text{ on } \partial\Omega.$$

The weak formulation of this is (1.2) with  $V := H_0^1(\Omega)$ ,  $a(u, v) = (\nabla u, \nabla v)_{L^2(\Omega)}$ , and  $b(u, v) = (u, v)_{L^2(\Omega)}$ .

**3.1. Preliminary.** Some notation on the discrete level is fixed throughout the remaining parts of this paper before the HHO eigensolver is presented.

**3.1.1. Triangulation.** Let  $\mathcal{M}$  be a finite collection of closed *convex* polytopes of positive volume with overlap of volume measure zero that cover  $\overline{\Omega} = \cup_{K \in \mathcal{M}} K$ . A side  $S$  of the mesh  $\mathcal{M}$  is a closed connected subset of a hyperplane  $H_S$  with positive  $(n-1)$ -dimensional surface measure such that either (a) there exist  $K_+, K_- \in \mathcal{M}$  with  $S \subset H_S \cap K_+ \cap K_-$  (interior side) or (b) there exists  $K_+ \in \mathcal{M}$  with  $S \subset H_S \cap K_+ \cap \partial\Omega$  (boundary sides). Let  $\Sigma$  be a finite collection of sides with overlap of  $(n-1)$ -dimensional surface measure zero that covers the skeleton  $\partial\mathcal{M} := \cup_{K \in \mathcal{M}} \partial K = \cup_{S \in \Sigma} S$ . The normal vector  $\nu_S$  of an interior side  $S \in \Sigma(\Omega)$  is fixed beforehand and set  $\nu_S := \nu|_S$  for boundary sides  $S \in \Sigma(\partial\Omega)$ . For  $S \in \Sigma(\Omega)$ ,  $K_+ \in \mathcal{M}$  (resp.  $K_- \in \mathcal{M}$ ) denotes the unique cell with  $S \subset \partial K_+$  (resp.  $S \subset \partial K_-$ ) and  $\nu_{K_+}|_S = \nu_S$  (resp.  $\nu_{K_-}|_S = -\nu_S$ ). The jump  $[v]_S$  of any function  $v \in W^{1,1}(\text{int}(T_+ \cup T_-); \mathbb{R}^m)$  along  $S \in \Sigma(\Omega)$  is defined by  $[v]_S := v|_{K_+} - v|_{K_-} \in L^1(S; \mathbb{R}^m)$ . If  $S \in \Sigma(\partial\Omega)$ , then  $[v]_S := v|_S$ . The set  $H^1(\mathcal{M})$  is the space of all piecewise  $H^1$  function with respect to the mesh  $\mathcal{M}$ . The notation  $\nabla_{pw}$  denotes the piecewise application of the differential operator  $\nabla$  without explicit reference to  $\mathcal{M}$ . This notation applies to other differential operators as well.

**3.1.2. Trace inequality.** Given a convex polyhedra  $K$ , let  $x_K$  denote the midpoint of  $K$ . For any side  $S \in \Sigma(K)$  of  $K$ , the simplex  $K_S := \text{conv}\{x_K, S\} \subset K$  is the convex hull of  $S$  and  $x_K$ . We define the weight

$$(3.2) \quad \ell(S, K) := |S|h_K^2/|K_S|.$$

Notice the scaling  $\ell(S, K) \approx h_K$  for admissible meshes (cf. [14, Definition 1.38] for a precise definition). This paper utilizes the following trace inequality.

**Lemma 3.1** (trace inequality). *Any  $v \in H^1(\text{int}(K))$  with  $\int_K v \, dx = 0$  satisfies*

$$\sum_{S \in \Sigma(K)} \ell(S, K)^{-1} \|v\|_{L^2(S)}^2 \leq c_{\text{tr}} \|\nabla v\|_{L^2(K)}^2$$

with the constant  $c_{\text{tr}} := 1/\pi^2 + 2/(n\pi)$ .

*Proof.* Given  $S \in \Sigma(K)$ , the classical trace identity implies

$$(3.3) \quad \|v\|_{L^2(S)}^2 \leq \frac{|S|}{|K_S|} \|v\|_{L^2(K_S)}^2 + \frac{2h_{K_S}|S|}{n|K_S|} \int_{K_S} |v| |\nabla v| \, dx$$

cf., e.g., [20, proof of Lemma 7.2]. The sum of this over all  $S \in \Sigma(K)$  with the notation  $\ell(S, K)$  from (3.2) and  $h_{K_S} \leq h_K$  establish

$$\sum_{S \in \Sigma(K)} \ell(S, K)^{-1} \|v\|_{L^2(S)}^2 \leq h_K^{-2} \|v\|_{L^2(K)}^2 + 2h_K^{-1} n^{-1} \int_K |v| |\nabla v| \, dx.$$

This, the Hölder, and Poincaré inequality conclude the proof.  $\square$

**3.1.3. Finite element spaces.** Given a subset  $M \subset \mathbb{R}^n$  of diameter  $h_M$ , let  $P_k(M)$  denote the space of polynomials of degree at most  $k$ . For any  $v \in L^1(M)$ ,  $\Pi_M^k v \in P_k(M)$  denotes the  $L^2$  projection of  $v$  onto  $P_k(M)$ . The space of piecewise polynomials of degree at most  $k$  with respect to the mesh  $\mathcal{M}$  or the sides  $\Sigma$  is denoted by  $P_k(\mathcal{M})$  or  $P_k(\Sigma)$ . Given  $v \in L^1(\Omega)$ , define the  $L^2$  projections  $\Pi_{\mathcal{M}}^k v$  and  $\Pi_{\Sigma}^k v$  of  $v$  onto  $P_k(\mathcal{M})$  and  $P_k(\Sigma)$  by  $(\Pi_{\mathcal{M}}^k v)|_K = \Pi_K^k v|_K$  in any cell  $K \in \mathcal{M}$  and  $(\Pi_{\Sigma}^k v)|_S = \Pi_S^k v$  along any side  $S \in \Sigma$ . The mesh  $\mathcal{M}$  gives rise to the piecewise constant function  $h_{\mathcal{M}} \in P_0(\mathcal{M})$  with  $h_{\mathcal{M}}|_K = h_K$ ;  $h_{\max} := \max_{K \in \mathcal{M}} h_K$  is the maximal mesh-size of  $\mathcal{M}$ .

**3.2. HHO eigensolver.** This subsection presents the HHO eigensolver for the computation of LEB. Let  $V_{\text{nc}} := H^1(\mathcal{M})$ ,  $a_{\text{pw}}(u_{\text{nc}}, v_{\text{nc}}) := (\nabla_{\text{pw}} u_{\text{nc}}, \nabla_{\text{pw}} v_{\text{nc}})_{L^2(\Omega)}$ , and  $W_{\text{nc}} := P_{k+1}(\mathcal{M})$ .

**3.2.1. Discrete ansatz spaces.** Given a fixed  $k \geq 0$ , let  $V_h := P_{k+1}(\mathcal{M}) \times P_k(\Sigma(\Omega))$  denote the discrete ansatz space for  $V$ . In this definition,  $P_k(\Sigma(\Omega))$  is the subspace of  $P_k(\Sigma)$  with the convention  $v_{\Sigma} \in P_k(\Sigma(\Omega))$  if  $v_{\Sigma}|_S \equiv 0$  on boundary sides  $S \in \Sigma(\partial\Omega)$  to model homogenous Dirichlet boundary condition. For any  $v_h = (v_{\mathcal{M}}, v_{\Sigma}) \in V_h$ , we use the notation  $v_K := v_{\mathcal{M}}|_K$  and  $v_S := v_{\Sigma}|_S$  to abbreviate the restriction of  $v_{\mathcal{M}}$  in a cell  $K \in \mathcal{M}$  and  $v_{\Sigma}$  along a side  $S \in \Sigma$ . The interpolation operator  $I_h : V \rightarrow V_h$  maps  $v \in V$  to  $I_h v := (\Pi_{\mathcal{M}}^k v, \Pi_{\Sigma}^k v) \in V_h$ .

**3.2.2. Reconstruction operators and stabilization.** We recall the potential reconstruction from [16].

*Potential reconstruction.* Given  $v_h = (v_{\mathcal{M}}, v_{\Sigma}) \in V_h$ , the potential reconstruction  $\mathcal{R}_h v_h \in W_{\text{nc}}$  satisfies, for any  $\varphi_{k+1} \in W_{\text{nc}}$ , that

$$(3.4) \quad a_{\text{pw}}(\mathcal{R}_h v_h, \varphi_{k+1}) = -(v_{\mathcal{M}}, \Delta_{\text{pw}} \varphi_{k+1})_{L^2(\Omega)} + \sum_{S \in \Sigma} (v_S, [\nabla_{\text{pw}} \varphi_{k+1}]_S)_{L^2(S)}.$$

This defines  $\mathcal{R}_h v_h$  uniquely up to piecewise constants, which is fixed by

$$(3.5) \quad \int_K \mathcal{R}_h v_h \, dx = \int_K v_K \, dx \quad \text{for any } K \in \mathcal{M}.$$

*Stabilization.* Given  $K \in \mathcal{M}$  and a positive parameter  $\sigma > 0$ , the stabilization  $s_K(u_h, v_h)$  reads, for any  $u_h = (u_{\mathcal{M}}, u_{\Sigma}), v_h = (v_{\mathcal{M}}, v_{\Sigma}) \in V_h$ ,

$$(3.6) \quad s_K(u_h, v_h) := \sigma h_K^{-2} (u_K - \mathcal{R}_h u_h, v_K - \mathcal{R}_h v_h)_{L^2(K)} + \sigma \sum_{S \in \Sigma(K)} \ell(S, K)^{-1} (\Pi_S^k(u_S - \mathcal{R}_h u_h|_K), v_S - \mathcal{R}_h v_h|_K)_{L^2(S)}$$

with  $\ell(S, K)$  from (3.2) and the global version  $s_h(u_h, v_h) := \sum_{K \in \mathcal{M}} s_K(u_h, v_h)$ . A similar stabilization has been proposed (and analysed) in [13, Example 2.8] for the discrete ansatz space  $P_k(\mathcal{M}) \times P_k(\Sigma(\Omega))$ , however we note that it is not sufficient for stability for the present ansatz space.

*Discrete eigenvalue problem.* The discrete eigenvalue problem (1.5) is defined with

$$(3.7) \quad a_h(u_h, v_h) := a_{\text{pw}}(\mathcal{R}_h u_h, \mathcal{R}_h v_h) \quad \text{and} \quad b_h(u_h, v_h) = (u_{\mathcal{M}}, v_{\mathcal{M}})_{L^2(\Omega)}$$

for any  $u_h = (u_{\mathcal{M}}, u_{\Sigma}), v_h = (v_{\mathcal{M}}, v_{\Sigma}) \in V_h$ . It is straightforward to verify the following result.

**Lemma 3.2** (coercivity). *The bilinear form  $a_h + s_h$  is a scalar product in  $V_h$ . In particular, there are  $\dim(P_{k+1}(\mathcal{M}))$  finite discrete eigenvalues of (1.5).*  $\square$

**3.3. Lower eigenvalue bounds.** This subsection verifies (A)–(C) as outlined in Subsection 1.3 and derives LEB for the Laplace operator. The Galerkin projection is defined by (1.8)–(1.9).

**Corollary 3.3** (LEB for Laplacian). *It holds*

$$\text{LEB}(j) := \min\{1, 1/(\sigma/\pi^2 + \sigma c_{\text{tr}} + h_{\max}^2 \lambda_h(j)/\pi^2)\} \lambda_h(j) \leq \lambda(j).$$

*Proof.* Given  $v \in V$ , the property  $G_h v = \mathcal{R}_h I_h v$  in (1.7) follows from the orthogonality  $v - \mathcal{R}_h I_h v \perp_{a_{\text{pw}}} W_{\text{nc}}$  [16, Eq. (18)] and  $\Pi_{\mathcal{M}}^0 \mathcal{R}_h I_h v = \Pi_{\mathcal{M}}^0 v$  in (3.5). Hence, any  $v \in V$  satisfies the Pythagoras theorem

$$\|I_h v\|_a^2 = \|v\|_a^2 - \|v - G_h v\|_{a_{\text{pw}}}^2.$$

This is (A). Fix a cell  $K \in \mathcal{M}$ . The best approximation property of the  $L^2$  projections and (1.7) provide the upper bound

$$\begin{aligned} & \sigma h_K^{-2} \|\Pi_K^{k+1}(v - G_h v)\|_{L^2(K)}^2 + \sigma \sum_{S \in \Sigma(K)} \ell(S, K)^{-1} \|\Pi_S^k(v - G_h v|_K)\|_{L^2(S)}^2 \\ & \leq \sigma h_K^{-2} \|v - G_h v\|_{L^2(K)}^2 + \sigma \sum_{S \in \Sigma(K)} \ell(S, K)^{-1} \|v - G_h v|_K\|_{L^2(S)}^2 \end{aligned}$$

for the stabilization  $s_K(I_h v, I_h v)$ . This, the Poincaré, and the trace inequality from Lemma 3.1 establish

$$(3.8) \quad \|I_h v\|_{s_h}^2 \leq (\sigma/\pi^2 + \sigma c_{\text{tr}}) \|v - G_h v\|_{a_{\text{pw}}}^2,$$

which is (B) with  $\alpha := (\sigma/\pi^2 + \sigma c_{\text{tr}})$ . The Pythagoras theorem and the best-approximation property of the  $L^2$  projection prove

$$(3.9) \quad \|I_h v\|_b^2 = \|\Pi_{\mathcal{M}}^{k+1} v\|^2 = \|v\|^2 - \|(1 - \Pi_{\mathcal{M}}^{k+1})v\|^2 \geq \|v\|^2 - \|(1 - G_h)v\|^2.$$

This and the Poincaré inequality show (C) with  $\beta := h_{\max}^2/\pi^2$ . Theorem 2.1 concludes the proof with the constants  $\alpha, \beta$  from above.  $\square$

**3.4. Numerical example.** The computer experiments throughout this paper are carried out on regular simplicial meshes. Some general remarks on the realization precede the numerical results.

**3.4.1. Parameter choice.** We chose  $\sigma := 2^{-1}(\pi^{-2} + c_{\text{tr}})^{-1} = 0.9598$  in Corollary 3.3, which provides  $\text{LEB}(j) = \min\{1, 1/(1/2 + h_{\max}^2 \lambda_h(j)/\pi^2)\} \lambda_h(1) \leq \lambda(1)$ .

**3.4.2. Displayed quantities.** The convergence history plots display the error  $\lambda_C(j) - \text{LEB}(j)$  against the number of degrees of freedom ndof in a log-log plot, where the upper bound  $\lambda_C(j)$  is the Rayleigh quotient of some conforming function  $u_C(j) \in P_{k+1}(\mathcal{M}) \cap V$ . If  $j = 1$ , then  $u_C(j)$  is the scaled nodal average of  $\mathcal{R}_h u_h(j)$  with  $\|u_C\|_b = 1$  and for  $j \geq 1$ ,  $u_C(j)$  can be obtained from the conforming Galerkin  $P_{k+1}$  FEM on the same mesh. At least on regular simplicial meshes (without hanging nodes),  $\|\mathbf{I}_h v_C\|_{a_h}^2 + \|\mathbf{I}_h v_C\|_{s_h}^2 = \|v_C\|_a^2$  and  $\|\mathbf{I}_h v_C\|_{b_h}^2 = \|v_C\|_b^2$  holds for any  $v_C \in P_{k+1}(\mathcal{M}) \cap V$ . Therefore, the discrete Rayleigh-Ritz principle (1.6) shows  $\lambda_h(j) \leq \lambda_C(j)$ . In combination with Theorem 2.1,  $\text{LEB}(j) \leq \{\lambda, \lambda_h(j)\} \leq \lambda_C(j)$  and so,  $|\lambda(j) - \lambda_h(j)| \leq \lambda_C(j) - \text{LEB}(j)$ .

**3.4.3. Adaptive refinement indicator.** For  $\text{LEB}(j) = \lambda_h(j)$ , the error estimator  $\lambda_C(j) - \lambda_h(j)$  can be localized following [23, Lemma 6.3]. Let  $u_C(j)$  be given such  $\lambda_C(j) = \|u_C\|_a^2$  with the normalization  $\|u_C(j)\|_b^2 = 1$  and  $(u_C(j), u_{\mathcal{M}}(j))_{L^2(\Omega)} > 0$ , where  $u_h(j) = (u_{\mathcal{M}}(j), u_{\Sigma}(j)) \in V_h$  is the computed eigenvector of  $\lambda_h(j)$ . Elementary algebra with  $\|\mathcal{R}_h u_h(j)\|_{a_{\text{pw}}}^2 = \lambda_h(j) - \|u_h(j)\|_{s_h}^2$  shows

$$\begin{aligned} \lambda_C(j) - \lambda_h(j) &= \|u_C(j)\|_a^2 - \lambda_h(j) \\ &= \|u_C(j) - \mathcal{R}_h u_h(j)\|_{a_{\text{pw}}}^2 + 2a_{\text{pw}}(u_C(j), \mathcal{R}_h u_h(j)) - \|\mathcal{R}_h u_h(j)\|_{a_{\text{pw}}}^2 - \lambda_h(j) \\ &= \|u_C(j) - \mathcal{R}_h u_h(j)\|_{a_{\text{pw}}}^2 + 2a_{\text{pw}}(u_C(j), \mathcal{R}_h u_h(j)) - 2\lambda_h(j) + \|u_h(j)\|_{s_h}^2. \end{aligned}$$

The discrete variational formulation (1.5) and the commuting property (1.7) show

$$\begin{aligned} 2a_{\text{pw}}(u_C(j), \mathcal{R}_h u_h(j)) &= 2\lambda_h(u_{\mathcal{M}}, u_C(j))_{L^2(\Omega)} \\ &= -\lambda_h \|u_C(j) - u_{\mathcal{M}}(j)\|_{L^2(\Omega)}^2 + \lambda_h (\|u_C\|_b^2 + \|u_h(j)\|_{b_h}^2). \end{aligned}$$

The combination of the two previously displayed formula with  $\|u_C\|_b^2 + \|u_h(j)\|_{b_h}^2 = 2$  concludes

$$(3.10) \quad \lambda_C(j) - \lambda_h(j) \leq \eta := \|u_C(j) - \mathcal{R}_h u_h(j)\|_{a_{\text{pw}}}^2 + \|u_h(j)\|_{s_h}^2.$$

Notice that the term  $-\lambda_h \|u_C(j) - u_{\mathcal{M}}(j)\|_{L^2(\Omega)}^2 \leq 0$  is neglected in the last formula. However, it is expected that  $\|u_C(j) - u_{\mathcal{M}}(j)\|_{L^2(\Omega)}^2$  is of higher order due to additional smoothness of the exact eigenvector. A generalization of (3.10) to general polyhedral meshes is possible with the addition of  $\|\mathbf{I}_h u_C\|_{s_h}^2$  on the right-hand side of (3.10). The bound (3.10) motivates the local refinement indicator

$$\eta(K) := \|\nabla_{\text{pw}}(u_C(j) - \mathcal{R}_h u_h(j))\|_{L^2(K)}^2 + s_K(u_h(j), u_h(j)).$$

This localization is relevant for simple eigenvalues. For the approximation of eigenvalue clusters, we suggest the use of residual-based error estimators, e.g., from [7], as in [19].

**3.4.4. Adaptive algorithm.** Whenever  $\alpha + \beta\lambda_h(j) > 1$ , the mesh is refined uniformly. Otherwise, the refinement indicator is utilized in the standard Dörfler marking with bulk parameter  $1/2$ , i.e., at each refinement step, a subset  $\mathfrak{M} \subset \mathcal{M}$  of minimal cardinality is selected so that

$$\eta \leq \frac{1}{2} \sum_{K \in \mathfrak{M}} \eta(K).$$

**3.4.5. Computer benchmark.** This benchmark approximates the first Dirichlet eigenvalue in the L-shaped domain  $\Omega := (-1, 1) \setminus ([0, 1] \times [-1, 0])$  with the reference value  $\lambda(1) = 9.63972384$  from the bound  $\text{LEB}(1) \leq \lambda(1) \leq \lambda_C(1)$ . The observations in this example also applies to all other benchmarks in Section 4–5 below. Figure 1(a) displays the convergence history of  $\lambda_C(1) - \text{LEB}(1)$ . Uniform mesh refinements leads to the suboptimal convergence rates  $2/3$  due to the expected singularity of the first eigenvector. Adaptive mesh computation refines towards the



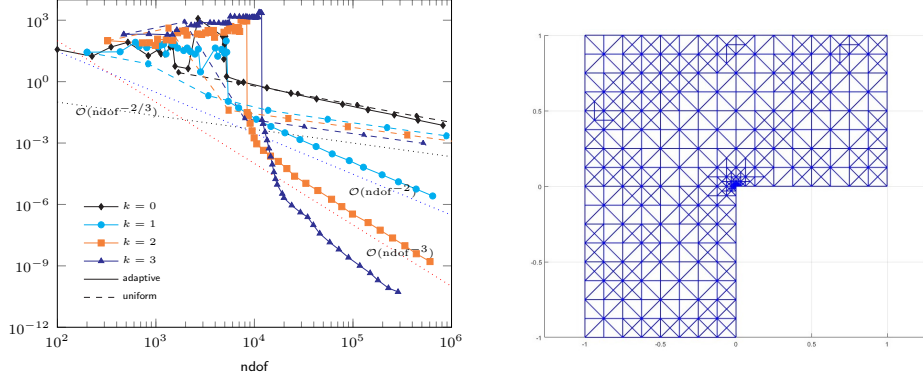


FIGURE 1. (a) convergence history plot of  $\lambda_C(1) - \text{LEB}(1)$  and (b) adaptive mesh with 736 triangles ( $k = 2$ ) for the Dirichlet eigenvalue problem in Subsection 3.4.5

origin as shown in Figure 1(b) and recovers the optimal convergence rates  $k + 1$  for all displayed polynomial degrees  $k$ . Undisplayed numerical experiments show that there are only marginal differences between  $\eta$  and  $\lambda_C(1) - \text{LEB}(1)$  except on very coarse meshes. Notice that Figure 1 also clearly displays a disadvantage of this method in comparison to other numerical schemes [22, 6, 20] with postprocessed eigenvalue bounds. The constants in local compact embeddings (e.g., trace inequalities) provide an upper bound for  $\sigma$  so that  $\alpha < 1$ . Since overestimation of these constants is expected,  $\sigma$  may be rather small in comparison to the best possible value with direct impact on the numerical method. We observe a preasymptotic range, where the discrete eigenvalue and lower bound are close to zero (and thus, not relevant) until the stabilization is resolved. A remedy is the computation of accurate upper bounds of the involved constants; we refer to Section 6 for further details.

#### 4. STEKLOV EIGENVALUE PROBLEM

The Steklov eigenvalue problem seeks eigenpairs  $(\lambda, u)$  with

$$-\Delta u + u = 0 \text{ in } \Omega \quad \text{and} \quad \partial u / \partial \nu = \lambda u \text{ on } \partial \Omega.$$

The weak formulation of this is (1.2) with  $V := H^1(\Omega)$ ,  $a(u, v) := (\nabla u, \nabla v)_{L^2(\Omega)} + (u, v)_{L^2(\Omega)}$ , and  $b(u, v) := (u, v)_{L^2(\partial \Omega)}$ .

**4.1. HHO eigensolver.** Let  $V_{\text{nc}} := H^1(\mathcal{M})$ ,  $a_{\text{pw}}(u_{\text{nc}}, v_{\text{nc}}) := (\nabla_{\text{pw}} u_{\text{nc}}, \nabla_{\text{pw}} v_{\text{nc}})_{L^2(\Omega)}$ , and  $W_{\text{nc}}(\mathcal{M}) := P_{k+1}(\mathcal{M})$  with  $k \geq 0$ . We utilize the discrete ansatz space  $V_h := P_k(\mathcal{M}) \times P_{k+1}(\Sigma)$  with the interpolation  $I_h v := (\Pi_{\mathcal{M}}^k v, \Pi_{\Sigma}^{k+1} v) \in V_h$  for any  $v \in V$ . The discrete problem (1.5) is defined with the bilinear forms

$$\begin{aligned} a_h(u_h, v_h) &:= (\nabla_{\text{pw}} \mathcal{R}_h u_h, \nabla_{\text{pw}} \mathcal{R}_h v_h)_{L^2(\Omega)} + (u_{\mathcal{M}}, v_{\mathcal{M}})_{L^2(\Omega)}, \\ b_h(u_h, v_h) &:= (u_{\Sigma}, v_{\Sigma})_{L^2(\partial \Omega)}, \end{aligned}$$

and the stabilization  $s_h(u_h, v_h) := \sum_{K \in \mathcal{M}} s_K(u_h, v_h)$ ,

$$\begin{aligned} s_K(u_h, v_h) &:= \sigma h_K^{-2} (\Pi_K^k (u_K - \mathcal{R}_h u_h), v_K - \mathcal{R}_h v_h)_{L^2(\Omega)} \\ &\quad + \sigma \sum_{S \in \Sigma(K)} \ell(S, K)^{-1} (u_S - \mathcal{R}_h u_h|_K, v_S - \mathcal{R}_h v_h|_K)_{L^2(S)}, \end{aligned}$$

for any  $u_h = (u_{\mathcal{M}}, u_{\Sigma}), v_h = (v_{\mathcal{M}}, v_{\Sigma}) \in V_h$ , where the potential reconstruction  $\mathcal{R}_h$  is defined verbatim as in (3.4)–(3.5). It is straightforward to verify the coercivity of  $a_h + s_h$ .

**Lemma 4.1** (coercivity). *The bilinear form  $a_h + s_h$  is a scalar product in  $V_h$ . In particular, there are  $\dim(P_{k+1}(\Sigma(\partial\Omega)))$  finite discrete eigenvalues of (1.5).  $\square$*

**4.2. Lower eigenvalue bounds.** This subsection verifies (A)–(C) and derives LEB for the Steklov eigenvalue problems. The Galerkin projection is defined by (1.8)–(1.9). We utilize the following trace inequality. Given a boundary side  $S \in \Sigma(\partial\Omega)$ , there exists a unique cell  $K \in \mathcal{M}$  with  $S \in \Sigma(K)$ . The largest simplex inscribed in  $K$  with the side  $S$  is denoted by  $K_S^m$ . (Notice that  $K_S^m = K$  for simplicial meshes.) The trace inequality (3.3) in  $K_S^m$  and a Hölder inequality provide, for any  $v \in H^1(K)$ , that

$$(4.1) \quad \|v\|_{L^2(S)}^2 \leq \frac{|S|}{|K_S^m|} \|v\|_{L^2(K)}^2 + \frac{2h_{K_S^m}|S|}{n|K_S^m|} \|v\|_{L^2(K)} \|\nabla v\|_{L^2(K)}.$$

This motivates the definition of the constant

$$(4.2) \quad \beta_{\text{St}} := c_0 \max_{S \in \Sigma(\partial\Omega)} \frac{h_K|S|}{|K_S^m|} (h_K/\pi^2 + 2h_{K_S^m}/(n\pi))$$

utilized in Corollary 4.2 below, where  $c_0$  is the maximal number of boundary sides belonging to the same cell.

**Corollary 4.2** (LEB for Steklov). *It holds*

$$(4.3) \quad \text{LEB}(j) := \min\{1, 1/(\sigma/\pi^2 + \sigma c_{\text{tr}} + \beta_{\text{St}}\lambda_h(j))\} \leq \lambda(j).$$

*Proof.* The property (1.7) is independent of boundary data and holds here as well. This, the Pythagoras theorem with the orthogonality  $v - G_h v \perp_{a_{\text{pw}}} W_{\text{nc}}$ , and the best approximation property of  $\Pi_{\mathcal{M}}^k$  imply, for any  $v \in V$ , that

$$\begin{aligned} \|I_h v\|_{a_h}^2 &= \|G_h v\|_{a_{\text{pw}}}^2 + \|\Pi_{\mathcal{M}}^k v\|^2 \\ &= \|v\|_{a_{\text{pw}}}^2 - \|v - G_h v\|_{a_{\text{pw}}}^2 + \|\Pi_{\mathcal{M}}^k v\|^2 \leq \|v\|_a^2 - \|v - G_h v\|_{a_{\text{pw}}}^2, \end{aligned}$$

which is (A). The same arguments as in the proof of Corollary 3.3 provide (B) with  $\alpha := \sigma/\pi^2 + \sigma c_{\text{tr}}$ . For any boundary side  $S \in \partial\Omega$ , let  $K$  denote the unique cell with  $S \in \Sigma(K)$ . The Pythagoras theorem and the best approximation property of  $L^2$  projections imply

$$\|\Pi_S^{k+1} v\|_{L^2(S)}^2 = \|v\|_{L^2(S)}^2 - \|v - \Pi_S^{k+1} v\|_{L^2(S)}^2 \leq \|v\|_{L^2(S)}^2 - \|v - G_h v\|_{L^2(S)}^2.$$

Invoking the trace inequality (4.1) and the Poincaré inequality, we infer that

$$(4.4) \quad \|v - G_h v\|_{L^2(S)}^2 \leq \frac{h_K|S|}{|K_S^m|} (h_K/\pi^2 + 2h_{K_S^m}/(n\pi)) \|\nabla(v - G_h v)\|_{L^2(K)}^2.$$

The combination of the two previously displayed formula with an overlap argument results in

$$\|I_h v\|_{b_h}^2 = \|\Pi_{\Sigma}^{k+1} v\|_{L^2(\partial\Omega)}^2 \leq \|v\|_b^2 - \beta_{\text{St}} \|v - G_h v\|_{a_{\text{pw}}}^2,$$

whence (C) holds with  $\beta := \beta_{\text{St}}$ . Theorem 2.1 concludes the assertion.  $\square$

**4.3. Computer benchmark.** This benchmark approximates the first Steklov eigenvalue in the  $L$ -shaped domain  $\Omega := (-1, 1) \setminus ([0, 1] \times [-1, 0])$  with the reference value  $\lambda(1) = 0.34141604251$  from the bound  $\text{LEB}(1) \leq \lambda(1) \leq \lambda_C(1)$ . We set  $\sigma := 2^{-1}(\pi^{-2} + c_{\text{tr}})^{-1} = 0.9598$  so that  $\text{LEB}(1) = \min\{1, 1/(1/2 + \beta_{\text{St}}\lambda_h(1))\}\lambda_h(1) \leq \lambda(1)$  from Corollary 4.2. The computation of  $\lambda_C(1)$  and  $u_C(1)$  follows Subsection 3.4.5. For the first discrete eigenvalue  $u_h(1) = (u_{\mathcal{M}}(1), u_{\Sigma}(1))$ , the bound

$$\lambda_C(1) - \lambda_h(1) \leq \|u_C(1) - \mathcal{R}_h u_h(1)\|_{a_{\text{pw}}}^2 + \|u_C(1) - u_{\mathcal{M}}(1)\|_{L^2(\Omega)}^2 + \|u_h(1)\|_{s_h}^2$$

similar to (3.10) provides the refinement indicator by localization of the right-hand side. Figure 2 displays the convergence history of  $\lambda_C(1) - \lambda_h(1)$  and the observations

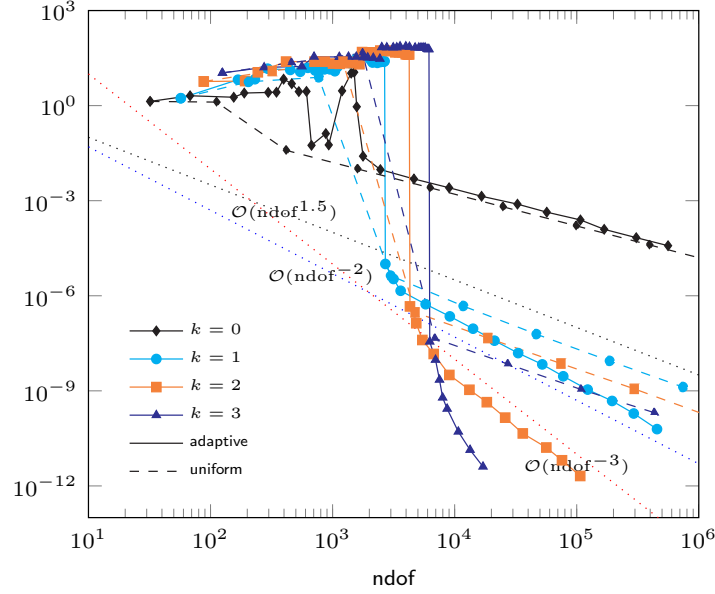


FIGURE 2. Convergence history plot of  $\lambda_C(1) - \text{LEB}(1)$  for the Steklov eigenvalue problem in Subsection 4.3

in Subsection 3.4.5 apply. An advantage of this method over [24, 20] is that, even for smooth eigenfunctions, the lower bounds therein can only converge towards the exact eigenvalue with the convergence rate  $1/2$  due to the scaling of the local compact embedding  $\|v\|_{L^2(S)}^2 \lesssim h_K \|v\|_{L^2(K)}^2$  for suitable  $v \in H^1(K)$ .

## 5. LINEAR ELASTICITY

Let the boundary  $\partial\Omega$  of  $\Omega$  be split into a closed connected nonempty Dirichlet part  $\Gamma_D \subset \partial\Omega$  and a Neumann part  $\Gamma_N := \partial\Omega \setminus \Gamma_D$ . The linear elasticity eigenvalue problem seeks eigenpairs  $(\lambda, u)$  such that

$$(5.1) \quad -\operatorname{div} \sigma = \lambda u \text{ in } \Omega, \quad \sigma = \mathbb{C}\varepsilon(u), \quad u = 0 \text{ on } \Gamma_D, \quad \text{and } \sigma\nu = 0 \text{ on } \Gamma_N.$$

Here,  $\varepsilon(v) := \operatorname{sym}(Dv)$  is the symmetric part of the gradient  $Dv$  of  $v$  and  $\mathbb{C}A := 2\mu A + \kappa \operatorname{tr}(A)\mathbb{I}_n$  for any  $A \in \mathbb{S}$  denotes the linearized strain tensor with Lamé parameters  $\lambda, \mu > 0$ . The weak formulation of (5.1) is (1.2) with  $V := \{v \in H^1(\Omega)^n : v = 0 \text{ on } \Gamma_D\}$ ,  $a(u, v) := (\mathbb{C}\varepsilon(u), \varepsilon(v))_{L^2(\Omega)}$ , and  $b(u, v) := (u, v)_{L^2(\Omega)}$ .

**5.1. HHO eigensolver.** Assume that the Dirichlet boundary can be exactly resolved by the mesh  $\mathcal{M}$ . Let  $V_{\text{nc}} := H^1(\mathcal{M})^n$ ,  $a_{\text{pw}} := (\mathbb{C}\varepsilon_{\text{pw}}(\bullet), \varepsilon_{\text{pw}}(\bullet))_{L^2(\Omega)}$ , and  $W_{\text{nc}} := P_{k+1}(\mathcal{M})^n$ . Given any  $k \geq 1$ ,  $V_h := P_{k+1}(\mathcal{M})^n \times P_k(\mathcal{M})^n$  denotes the discrete ansatz space. The potential reconstruction  $\mathcal{R}_h v_h \in W_{\text{nc}}$  of  $v_h = (v_{\mathcal{M}}, v_{\Sigma}) \in V_h$  satisfies, for any  $\varphi_{\text{nc}} \in W_{\text{nc}}$ , that

$$(5.2) \quad \begin{aligned} a_{\text{pw}}(\mathcal{R}_h v_h, \varphi_{\text{nc}}) &= -(v_{\mathcal{M}}, \operatorname{div}_{\text{pw}} \mathbb{C}\varepsilon_{\text{pw}}(\varphi_{\text{nc}}))_{L^2(\Omega)} \\ &\quad + \sum_{S \in \Sigma} (v_S, [\mathbb{C}\varepsilon_{\text{pw}}(\varphi_{\text{nc}})]_S \nu_S)_{L^2(S)}. \end{aligned}$$

This defines  $\mathcal{R}_h u_h$  uniquely up to the degrees of freedom associated with rigid body motions, which are fixed, for any  $K \in \mathcal{M}$ , by

$$(5.3) \quad \int_K \mathcal{R}_h v_h \, dx = \int_K v_K \, dx, \quad \int_K D_{\text{ss}} \mathcal{R}_h v_h \, dx = \sum_{S \in \Sigma(K)} \int_S \operatorname{asym}(\nu_K \otimes v_S) \, ds,$$

where  $D_{ss}$  denotes the asymmetric part of the gradient and  $\nu_K \otimes v_S := \nu_K v_S^t \in \mathbb{R}^{n \times n}$ . By design,  $\mathcal{R}_h$  satisfies the following.

**Lemma 5.1** (projection property). *Any  $v \in V$  satisfies the  $a_{pw}$  orthogonality  $v - \mathcal{R}_h I_h v \perp P_{k+1}(\mathcal{M})^n$ .*

*Proof.* For any  $\varphi_{nc} \in W_{nc}$ ,  $\text{div}_{pw} \mathbb{C} \varepsilon_{pw}(\varphi_{nc}) \in P_{k-1}(\mathcal{M})^n$  and  $[\mathbb{C} \varepsilon_{pw}(\varphi_{nc})]_S \nu_S \in P_k(S)^n$  along  $S \in \Sigma$ . By choosing  $v_h := I_h v$  in (5.2), we observe that  $v_{\mathcal{M}} = \Pi_{\mathcal{M}}^{k+1} v$  and  $v_S = \Pi_S^k v$  on the right-hand side of (5.2) can be replaced by  $v$ . A piecewise integration by parts of the resulting term shows  $(\mathbb{C} \varepsilon_{pw}(\mathcal{R}_h I_h v), \varepsilon_{pw}(\varphi_{nc}))_{L^2(\Omega)} = (\mathbb{C} \varepsilon(v), \varepsilon_{pw}(\varphi_{nc}))_{L^2(\Omega)}$ .  $\square$

The discrete problem (1.5) is defined with

$$a_h(u_h, v_h) := a_{pw}(\mathcal{R}_h u_h, \mathcal{R}_h v_h), \quad b_h(u_h, v_h) := (u_{\mathcal{M}}, v_{\mathcal{M}})_{L^2(\Omega)},$$

and  $s_h(u_h, v_h) := \sum_{K \in \mathcal{M}} s_K(u_h, v_h)$  with

$$\begin{aligned} s_K(u_h, v_h) &:= 2\mu\sigma \int_K h_K^{-2} (u_K - \mathcal{R}_h u_h) \cdot (v_K - \mathcal{R}_h v_h) \, dx \\ &\quad + 2\mu\sigma \sum_{S \in \Sigma(K)} \ell(S, K)^{-1} \int_S \Pi_S^k (u_S - \mathcal{R}_h u_h|_K) \cdot \Pi_S^k (v_S - \mathcal{R}_h v_h|_K) \, ds \end{aligned}$$

for any  $u_h = (u_{\mathcal{M}}, u_{\Sigma}), v_h = (v_{\mathcal{M}}, v_{\Sigma}) \in V_h$ , where  $\ell(S, K)$  is the weight from (3.2). It is straightforward to verify the coercivity of  $a_h + s_h$ .

**Lemma 5.2** (coercivity). *The bilinear form  $a_h + s_h$  is a scalar product in  $V_h$ . In particular, there are  $\dim(P_{k+1}(\mathcal{M}))$  finite discrete eigenvalues of (1.5).*  $\square$

**5.2. Lower eigenvalue bounds.** This subsection verifies (A)–(C) and derives LEB for the linear elasticity eigenvalue problem. The Galerkin projection  $G_h v \in W_{nc}$  of  $v \in V_{nc}$  is the unique solution to (1.8) with, for any  $K \in \mathcal{M}$ ,

$$(5.4) \quad \int_K G_h v \, dx = \int_K v \, dx \quad \text{and} \quad \int_K D_{ss} G_h v_h \, dx = \int_K D_{ss} v \, ds.$$

**Lemma 5.3** ( $\mathcal{R}_h \circ I_h = G_h$ ). *The identity (1.7) holds in  $V$ .*

*Proof.* Given  $v \in V$ , Lemma 5.1 implies that  $\mathcal{R}_h I_h v$  satisfies (1.8). For any  $K \in \mathcal{M}$ ,  $\int_K \mathcal{R}_h I_h v \, dx = \int_K \Pi_{\mathcal{M}}^{k+1} v \, dx = \int_K v \, dx$  and  $\sum_{S \in \Sigma(K)} \int_S \text{asym}(\nu_K \otimes \Pi_S^k v) \, ds = \sum_{S \in \Sigma(K)} \int_S \text{asym}(\nu_K \otimes v) \, ds = \int_K D_{ss} v \, dx$  from (5.3) and an integration by parts. Hence,  $\mathcal{R}_h I_h v = G_h v$ .  $\square$

Given  $K \in \mathcal{M}$ , let  $c_{\text{Korn}}(K)$  denote the Korn constant in the inequality

$$(5.5) \quad \|Dv\|_{L^2(K)} \leq c_{\text{Korn}}(K) \|\varepsilon(v)\|_{L^2(K)}$$

for any  $v \in H^1(K)^n$  with  $\int_K D_{ss} v \, dx = 0$  [3]. The computation of LEB for linear elasticity requires the following result in the local space  $V(K) := \{v \in H^1(K)^n : \int_K v \, dx = 0 \text{ and } \int_K D_{ss} v \, dx = 0\}$ .

**Lemma 5.4** (local embedding in linear elasticity). *Given a convex polyhedra  $K \subset \mathbb{R}^n$ , there exists a constant  $\gamma(K) \geq c_{\text{Korn}}^{-2}(K)(\pi^{-2} + c_{\text{st}})^{-1}$  with, for any  $v \in V(K)$ ,*

$$\sum_{S \in \Sigma(K)} \ell(S, K)^{-1} \|v\|_{L^2(S)}^2 + h_K^{-2} \|v\|_{L^2(K)}^2 \leq \gamma(K)^{-1} \|\varepsilon(v)\|_{L^2(K)}^2.$$

*The constant  $\gamma(K)$  may depend on the shape but not on the diameter of  $K$ .*

*Proof.* The assertion follows from Lemma 3.1, a Poincaré, and Korn inequality.  $\square$

Lemma 5.3–5.4 allow for the verification of (A)–(C) with the constants  $c_{\text{Korn}} := \max_{K \in \mathcal{M}} c_{\text{Korn}}(K)$  and  $\gamma := \max_{K \in \mathcal{M}} \gamma(K)$ .

**Corollary 5.5** (LEB for linear elasticity). *It holds*

$$\min\{1, 1/(\gamma^{-1}\sigma + c_{\text{Korn}}^2 h_{\max}^2 \lambda_h(j)/(2\pi^2 \mu))\} \lambda_h(j) \leq \lambda(j)$$

*Proof.* Given  $v \in V$ , the Pythagoras theorem with the  $a_{\text{pw}}$  orthogonality  $v - G_h v \perp P_{k+1}(\mathcal{M})^n$  from Lemma 5.1 and Lemma 5.3 proves (A), namely,

$$\|G_h v\|_{a_{\text{pw}}}^2 = \|v\|_a^2 - \|v - G_h v\|_{a_{\text{pw}}}^2$$

for any  $v \in V$ . Since  $v - Gv \in V(K)$  for any  $K \in \mathcal{M}$ , Lemma 5.3–5.4 and the best approximation property of  $L^2$  projections provide

$$\begin{aligned} s_K(I_h v, I_h v) &\leq 2\mu\sigma \sum_{S \in \Sigma(K)} \ell(S, K)^{-1} \|v - G_h v\|_{L^2(S)}^2 + 2\mu\sigma h_K^{-2} \|v - G_h v\|_{L^2(K)}^2 \\ (5.6) \quad &\leq 2\gamma(K)^{-1} \mu\sigma \|\varepsilon(v - G_h v)\|_{L^2(K)}^2. \end{aligned}$$

The sum of this over all  $K \in \mathcal{M}$  yields (B) with the constant  $\alpha := \gamma^{-1}\sigma$ . The combination of (3.9) with the Korn inequality (5.5) yields (C) with the constant  $\beta = c_{\text{Korn}}^2 h_{\max}^2 / (2\pi^2 \mu)$ . Theorem 2.1 concludes the proof.  $\square$

*Remark 5.6* ( $\kappa$  robustness). Utilizing the arguments of [10], we can prove the robustness of this method with respect to  $\kappa \rightarrow \infty$  on regular triangulations  $\mathcal{M}$  into simplices in the following sense. Given  $f \in L^2(\Omega)^n$ , let  $u \in V$  solve

$$-\text{div } \sigma = f \text{ in } \Omega, \quad \sigma = \mathbb{C}\varepsilon(u), \quad \sigma\nu = 0 \text{ on } \Gamma_N.$$

Then the discrete solution  $u_h \in V_h$  to  $a_h(u_h, v_h) + s_h(u_h, v_h) = (f, v_h)_{L^2(\Omega)}$  for any  $v_h = (v_{\mathcal{M}}, v_{\Sigma}) \in V_h$  satisfies

$$\begin{aligned} &\|\sigma - \sigma_h\|_{L^2(\Omega)} + \|I_h u - u_h\|_{a_h} + \|I_h u - u_h\|_{s_h} \\ &\lesssim \min_{p_{k+1} \in P_{k+1}(\mathcal{M})} \|\sigma - \mathbb{C}\varepsilon_{\text{pw}}(p_{k+1})\|_{L^2(\Omega)} + \text{osc}(f, \mathcal{M}), \end{aligned}$$

where  $\sigma_h := \mathbb{C}\varepsilon_{\text{pw}}(\mathcal{R}_h u_h)$  and  $\text{osc}(f, \mathcal{M}) := \|h_{\mathcal{M}}(1 - \Pi_{\mathcal{M}}^{k+1})f\|_{L^2(\Omega)}$ . The hidden constant in  $\lesssim$  is independent of  $\kappa$  and the mesh-size.

*Remark 5.7* (alternative eigensolver). The following alternative approach utilizes an additional reconstruction for the divergence as suggested in [15]. Given  $v_h = (v_{\mathcal{M}}, v_{\Sigma}) \in V_h$ , the divergence reconstruction  $\text{div}_h v_h \in P_k(\mathcal{M})$  uniquely solve

$$(\text{div}_h v_h, p_k)_{L^2(\Omega)} = -(v_{\mathcal{M}}, \nabla_{\text{pw}} p_k)_{L^2(\Omega)} + \sum_{S \in \Sigma} (v_S \cdot \nu_S, [p_k]_S)_{L^2(S)}$$

for any  $p_k \in P_k(\mathcal{M})$ . The discrete problem (1.5) is defined as in Subsection 5.1 with the following modifications:  $a_{\text{pw}}(u_{\text{nc}}, v_{\text{nc}}) := (\varepsilon_{\text{pw}}(u_{\text{nc}}), \varepsilon_{\text{pw}}(v_{\text{nc}}))_{L^2(\Omega)}$  and  $a_h$  is replaced by

$$a_h(u_h, v_h) := 2\mu a_{\text{pw}}(\mathcal{R}_h u_h, \mathcal{R}_h v_h)_{L^2(\Omega)} + \kappa (\text{div}_h u_h, \text{div}_h v_h)_{L^2(\Omega)},$$

where  $\mathcal{R}_h$  is the potential reconstruction from (6.2) below, similar to [15, Section 3.2]. For any  $v \in V$ , the  $a_{\text{pw}}$  orthogonality  $v - \mathcal{R}_h I_h v \perp P_{k+1}(\mathcal{M}; \mathbb{R}^n)$  [15, Eq. (19)] implies (1.7). This and the Pythagoras theorem with the  $L^2$  orthogonality  $\text{div}_h(v - I_h v) \perp P_k(\mathcal{M})$  [15, Proposition 3] shows (A) with

$$\begin{aligned} \|I_h v\|_{a_h}^2 &= 2\mu \|v\|_{a_{\text{pw}}}^2 - 2\mu \|v - G_h v\|_{a_{\text{pw}}}^2 + \kappa \|\text{div } v\|_{L^2(\Omega)}^2 - \kappa \|(1 - \Pi_{\mathcal{M}}^k) \text{div } v\|_{L^2(\Omega)}^2 \\ &\leq 2\mu \|v\|_a^2 - 2\mu \|v - G_h v\|_{a_{\text{pw}}}^2. \end{aligned}$$

The condition (B) follows from (5.6); (C) is a consequence of (3.9) and the Korn inequality (5.5). It turns out that (A)–(C) are valid with the same constants  $\alpha$  and  $\beta$  from Corollary 5.5, whence Corollary 5.5 holds verbatim.

In practice, the computation of the LEB in Corollary 5.5 requires an upper bound of the Korn constant in convex polyhedra. This is closely related to the continuity constant of a right-inverse of the divergence operator and is available in 2d from [12, 20]. For any  $K \in \mathcal{M}$ , let  $z_K$  be the midpoint of a largest ball inscribed in  $K$  with nodes  $x_1, \dots, x_m$ . Define the geometric parameter

$$\varrho(K) := \frac{\text{dist}(z_K, \partial K)}{\max_{j=1, \dots, m} |z_K - x_j|} \quad \text{and} \quad \varrho := \max_{K \in \mathcal{M}} \varrho(K),$$

then [20, Lemma 6.2] provides the upper bound

$$c_{\text{Korn}} \leq \sqrt{1 + \frac{4}{d^2} (1 + \sqrt{1 - d^2})}$$

of the Korn constant. For right-isosceles triangles,  $c_{\text{Korn}} \leq 7.318$ .

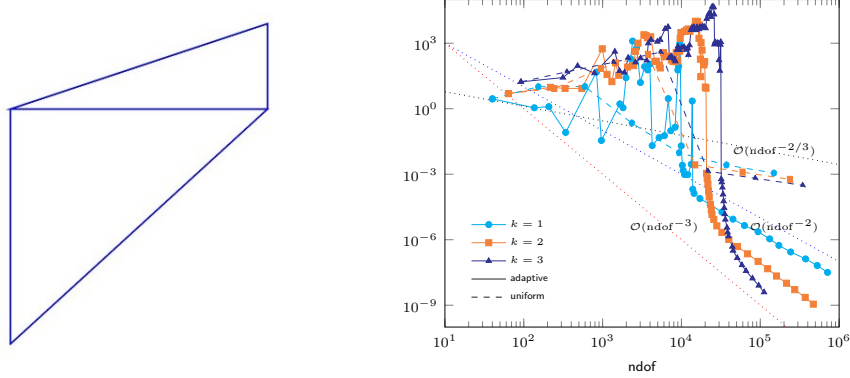


FIGURE 3. (a) initial triangulation and (b) convergence history plot of  $\lambda_C(1) - \text{LEB}(1)$  for the linear elasticity eigenvalue problem in Subsection 5.3

**5.3. Computer benchmark.** We approximate the first linear elasticity eigenvalue in the Cook's membrane  $\Omega := \text{conv}\{(0, 0), (48, 44), (48, 60), (0, 44)\}$  with the Dirichlet boundary  $\Gamma_D := \text{conv}\{(0, 0), (0, 44)\}$ , Neumann boundary  $\Gamma_N := \partial\Omega \setminus \Gamma_D$ , and parameters  $\mu = 1/2$  and  $\kappa = 1000$ . The initial triangulation of  $\Omega$  is displayed in Figure 3(a). The reference value  $\lambda(1) = 2.9020 \times 10^{-4}$  stems from the bound  $\text{LEB}(1) \leq \lambda(1) \leq \lambda_h(1)$ . We set  $\sigma := 2^{-1} c_{\text{Korn}}^{-2} (\pi^{-2} + c_{\text{tr}})^{-1} = 0.016049$  so that  $\min\{1, 1/(1/2 + c_{\text{Korn}}^2 h_{\max}^2 \lambda_h(j)/\pi^2)\} \lambda_h(j) \leq \lambda(j)$  from Corollary 5.5. The computation of  $\lambda_C(1)$  and  $u_C(1)$  follows Subsection 3.4.5. For the first discrete eigenvalue  $u_h(1) = (u_{\mathcal{M}}(1), u_{\Sigma}(1))$ , the bound

$$\lambda_C(1) - \lambda_h(1) \leq \|u_C(1) - \mathcal{R}_h u_h(1)\|_{a_{\text{pw}}}^2 + \|u_h(1)\|_{s_h}^2$$

similar to (3.10) motivates a refinement indicator by localization of the right-hand side. Figure 3(b) displays the convergence history of  $\lambda_C(1) - \text{LEB}(1)$  and the observations of Subsection 3.4.5 apply.

## 6. COMPACT EMBEDDING IN LINEAR ELASTICITY

The quality of lower eigenvalue bounds depends on the accuracy of constants in local embeddings. For the HHO eigensolvers of this paper however, they also directly influence the numerical scheme in the choice of  $\sigma$  for the stabilization. An overestimation in trace or Korn inequalities leads to inaccurate lower eigenvalue bounds on coarse meshes in all computer benchmarks of the previous three sections. This section proposes eigensolvers to compute improved guaranteed bounds of the relevant constants in Theorem 2.1, which can significantly reduce the size of the

preasymptotic range. Given a convex polyhedra  $\Omega$  of diameter  $d := \text{diam}(\Omega)$  and the set of sides  $\mathcal{E}$ , define the piecewise constant weight function  $\ell(\partial\Omega) \in P_0(\mathcal{E})$  by

$$\ell(\partial\Omega)|_S = \ell(S, \Omega) \quad \text{for any } S \in \mathcal{E}$$

with  $\ell(\Omega, S)$  from (3.2). We seek lower bounds  $\gamma_*(\Omega)$  of

$$(6.1) \quad \gamma(\Omega) = \min_{v \in V \setminus \{0\}} \|v\|_a^2 / \|v\|_b^2$$

in the space  $V = \{v \in H^1(\Omega)^n : \int_{\Omega} v \, dx = 0 \text{ and } \int_{\Omega} D_{ss} v \, dx = 0\}$  with

$$a(v, v) := (\varepsilon(v), \varepsilon(v))_{L^2(\Omega)} \quad \text{and} \quad b(v, v) := (\ell(\partial\Omega)^{-1} v, v)_{L^2(\partial\Omega)} + d^{-2}(v, v)_{L^2(\Omega)}.$$

Notice that  $\gamma(\Omega)^{-1}$  is the best possible constant in  $\|v\|_b^2 \leq \gamma(\Omega)^{-1} \|v\|_a^2$  for all  $v \in V$  and is utilized in Corollary 5.5 for LEB of the linear elasticity eigenvalue problem.

**6.1. HHO eigensolver.** For the problem (6.1) at hand, set  $V_{nc} := H^1(\mathcal{M})^n$ ,  $a_{pw}(u_{nc}, v_{nc}) := (\varepsilon_{pw}(u_{nc}), \varepsilon_{pw}(v_{nc}))_{L^2(\Omega)}$ , and  $W_{nc} := P_{k+1}(\mathcal{M})^n$ . For any  $v_h = (v_{\mathcal{M}}, v_{\Sigma}) \in P_{k+1}(\mathcal{M})^n \times P_{k+1}(\Sigma)^n$ , the potential reconstruction  $\mathcal{R}_h v_h \in W_{nc}$  of  $v_h$  from [15] satisfies, for any  $\varphi_{k+1} \in W_{nc}$ , that

$$(6.2) \quad \begin{aligned} & a_{pw}(\mathcal{R}_h v_h, \varphi_{k+1}) \\ &= -(v_{\mathcal{M}}, \text{div}_{pw} \varepsilon_{pw}(\varphi_{k+1}))_{L^2(\Omega)} + \sum_{S \in \Sigma} (v_S, [\varepsilon_{pw}(\varphi_{k+1})]_S \nu_S)_{L^2(S)}. \end{aligned}$$

This defines  $\mathcal{R}_h v_h$  uniquely up to rigid body motions. The associated degrees of freedom are fixed by (5.3). Given  $k \geq 0$ , let  $V_h := \{v_h = (v_{\mathcal{M}}, v_{\Sigma}) \in P_{k+1}(\mathcal{M})^n \times P_{k+1}(\Sigma)^n : \int_{\Omega} v_{\mathcal{M}} = 0 \text{ and } \int_{\Omega} D_{ss} \mathcal{R}_h v_h \, dx = 0\}$  denote the discrete ansatz space. Given  $v \in V$ , we claim that  $I_h v := (\Pi_{\mathcal{M}}^{k+1} v, \Pi_{\Sigma}^{k+1} v) \in V_h$ . In fact, the fixed degrees of freedom in (5.3) imply  $\int_K D_{ss} \mathcal{R}_h I_h v \, dx = \int_K D_{ss} v \, dx$  for any  $K \in \mathcal{M}$  in the proof of Lemma 5.3. Since  $\int_{\Omega} \Pi_{\mathcal{M}}^{k+1} v \, dx = 0$  from  $\int_{\Omega} v \, dx = 0$ , this shows

$$\int_{\Omega} D_{ss} \mathcal{R}_h I_h v \, dx = \int_{\Omega} D_{ss} v \, dx = 0$$

Therefore,  $I_h v \in V_h$  and so,  $I_h$  is an interpolation from  $V$  onto  $V_h$ . The discrete problem (1.5) is defined with the bilinear forms

$$\begin{aligned} a_h(u_h, v_h) &:= a_{pw}(\mathcal{R}_h u_h, \mathcal{R}_h v_h), \\ b_h(u_h, v_h) &:= (\ell(\partial\Omega)^{-1} u_{\Sigma}, v_{\Sigma})_{L^2(\partial\Omega)} + d^{-2}(u_{\mathcal{M}}, v_{\mathcal{M}})_{L^2(\Omega)}, \end{aligned}$$

and the stabilization  $s_h(u_h, v_h) := \sum_{K \in \mathcal{M}} s_K(u_h, v_h)$ ,

$$(6.3) \quad \begin{aligned} s_K(u_h, v_h) &:= \sigma \int_K h_K^{-2} (u_K - \mathcal{R}_h u_h) \cdot (v_K - \mathcal{R}_h v_h) \, dx \\ &+ \sigma \sum_{S \in \Sigma(K)} \ell(S, K)^{-1} \int_S (u_S - \mathcal{R}_h u_h|_K) \cdot (v_S - \mathcal{R}_h v_h|_K) \, ds \end{aligned}$$

for any  $u_h = (u_{\mathcal{M}}, u_{\Sigma}), v_h = (v_{\mathcal{M}}, v_{\Sigma}) \in V_h$ . It is straightforward to verify the following result.

**Lemma 6.1.** *The bilinear form  $a_h + s_h$  is a scalar product in  $V_h$ . In particular, there are  $\dim(P_{k+1}(\mathcal{M})) + \dim(P_{k+1}(\Sigma(\partial\Omega))) - M$  finite discrete eigenvalues of (1.5), where  $M$  is the number of rigid-body motions in  $n$ -d.  $\square$*

#	$\sigma$	$\gamma_*$
1	0.0358473	0.286114
2	0.286114	2.2488
3	2.2488	6.45254
4	6.45254	7.01185
5	7.01185	7.02938

TABLE 1. Lower bounds of  $\gamma$  for the reference triangle in Subsection 6.3

**6.2. Lower eigenvalue bounds.** The conditions (A)–(C) are verified in this subsection, which leads to LEB in Corollary 6.2 below. The Galerkin projection  $G_h v \in W_{nc}$  of  $v \in V_{nc}$  is defined by (1.8) with (5.4). Although the focus is on the first eigenvalue  $\lambda(1) = \gamma(\Omega)$ , LEB can be obtained for other eigenvalues  $\lambda(j)$  as well. Recall  $\gamma = \max_{K \in \mathcal{M}} \gamma(K)$  with  $\gamma(K)$  from Lemma 5.4.

**Corollary 6.2** (LEB in local embeddings). *It holds*

$$\text{LEB}(j) := \min\{1, \gamma/\sigma\} \lambda_h(j) \leq \lambda(j).$$

*Proof.* The verification of (1.7) is similar to Lemma 5.3, cf. also [15]. This provides (A) even with equality (instead of  $\leq$ ). Given  $v \in V$ , the identity

$$s_K(I_h v, I_h v) = \sigma \sum_{S \in \Sigma(K)} \ell(S, K)^{-1} \|v - G_h v\|_{L^2(S)}^2 + \sigma h_K^{-2} \|v - G_h v\|_{L^2(K)}^2$$

for any  $K \in \mathcal{M}$  from Lemma 5.3 and Lemma 5.4 imply (B) with  $\alpha = \gamma^{-1} \sigma$ . Since  $\ell(\partial\Omega)$  is piecewise constant, the Pythagoras theorem with the orthogonality of  $L^2$  projections establish

$$\begin{aligned} \|I_h v\|_{b_h}^2 &= \sum_{S \in \Sigma(\partial\Omega)} \ell(\partial\Omega)|_S^{-1} \|\Pi_\Sigma^{k+1} v\|_{L^2(S)}^2 + d^{-2} \|\Pi_{\mathcal{M}}^{k+1} v\|_{L^2(\Omega)}^2 \\ &= \|v\|_b^2 - \sum_{S \in \Sigma(\partial\Omega)} \ell(\partial\Omega)|_S^{-1} \|(1 - \Pi_\Sigma^{k+1})v\|_{L^2(S)}^2 + d^{-2} \|(1 - \Pi_{\mathcal{M}}^{k+1})v\|_{L^2(\Omega)}^2 \\ &\geq \|v\|_b^2 - \sum_{S \in \Sigma(\partial\Omega)} \ell(\partial\Omega)|_S^{-1} \|v - G_h v\|_{L^2(S)}^2 + d^{-2} \|v - G_h v\|_{L^2(\Omega)}^2 \end{aligned}$$

This, (4.4), the Poincaré, and Korn inequality show (C) with  $\beta = c_{\text{Korn}}^2 (h_{\max}^2/\pi^2 + \beta_{\text{st}})$ . The application of Theorem 2.1 yields

$$\min\{1, 1/(\gamma^{-1} \sigma + c_{\text{Korn}}^2 (h_{\max}^2/\pi^2 + \beta_{\text{st}}) \lambda_h(j))\} \lambda_h(j) \leq \lambda(j)$$

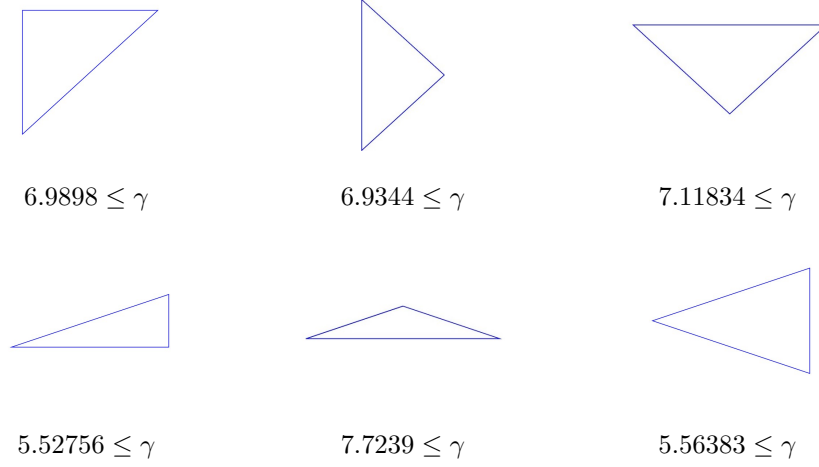
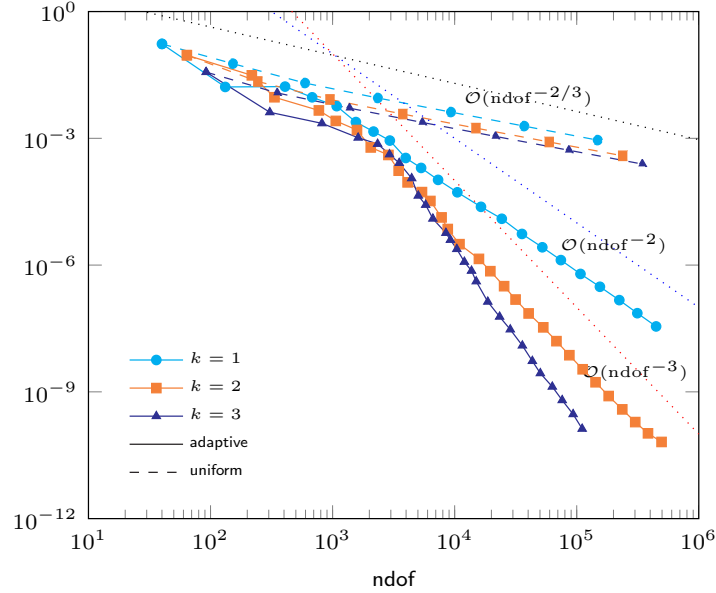
with  $\beta_{\text{st}}$  from (4.2). Given a positive parameter  $t > 0$ , consider the domain  $\Omega_t := t\Omega$  with the partition  $\mathcal{M}_t := \{tK : K \in \mathcal{M}\}$ . Since the continuous and discrete Rayleigh quotients are invariant under scaling, the continuous and discrete eigenvalue in  $\Omega_t$  coincide with those in  $\Omega$ . On the mesh  $\mathcal{M}_t$ , the arguments from above lead to the LEB

$$\min\{1, 1/(\gamma^{-1} \sigma + c_{\text{Korn}}^2 (t^2 h_{\max}^2/\pi^2 + t \beta_{\text{st}}) \lambda_h(j))\} \lambda_h(j) \leq \lambda(j)$$

due to the invariance of  $c_{\text{Korn}}$  and the scaling  $\beta_{\text{st}} \approx h_{\max}$ . The limit of this as  $t \rightarrow 0$  concludes the proof.  $\square$

**6.3. Computer benchmark.** Lower bounds  $\gamma_*(\Omega) = \text{LEB}(1)$  of  $\gamma(\Omega)$  in the reference triangle  $\Omega = \text{conv}\{(0,0), (1,0), (0,1)\}$  are computed on a fixed mesh  $\mathcal{M}$  created by three successive uniform refinements of the reference triangle, where each refinement divides every cell of  $\mathcal{M}$  into four congruent cells by connecting the mid points on the three sides. Notice that the constant  $\gamma(\Omega)$  is invariant under translation, scaling, and half rotation. Since every triangle in  $\mathcal{M}$  is the image of




 FIGURE 4. Lower bounds of  $\gamma$  for different triangular shapes in Subsection 6.4

 FIGURE 5. Improved convergence history plot of  $\lambda_C(1) - \text{LEB}(1)$  for the linear elasticity eigenvalue problem in Subsection 6.4

$\Omega$  under a combination of these transformations,  $\gamma(K) = \gamma(\Omega)$  for all  $K \in \mathcal{M}$  in Lemma 5.4. This leads to

$$(6.4) \quad \gamma_*(\Omega) = \min\{1, \gamma(\Omega)/\sigma\} \lambda_h(1) \leq \gamma(\Omega)$$

in Corollary 6.2. We set  $\sigma := c_{\text{Korn}}^{-2}(\pi^{-2} + c_{\text{tr}})^{-1} = 0.0358473 \leq \gamma(\Omega)$  so that  $\lambda_h(j) \leq \lambda(j)$  in (6.4). From the numerical experiments in the previous section, only rough bounds can be expected. For the choice  $k = 1$ , we obtain the lower bound  $\gamma_*(\Omega) = 0.286114$ . (For reference,  $\gamma \geq 7$  below.) Since the computed lower bound  $\gamma_*(\Omega)$  is larger than the initial bound  $c_{\text{Korn}}^{-2}(\pi^{-2} + c_{\text{tr}})^{-1} = 0.0358473$ , we repeat the computation with  $\sigma = \gamma_*(\Omega) = 0.286114$ . This process can be successively repeated by updating  $\sigma = \gamma_*(\Omega)$  after each iteration. Table 1 displays the computed lower bounds and provides  $7 \leq \gamma(\Omega)$  in the reference triangle.

**6.4. A revisit to linear elasticity.** In the setting of Subsection 5.3, we compute the lower bounds of  $\gamma(K)$  for all possible triangles  $K$  that can occur from the newest vertex bisection as described in Subsection 6.3. For the initial triangulation of the Cook's membrane displayed in Figure 3(a), lower bounds needs to be computed in six different triangles due to invariance of  $\gamma(K)$  under scaling, translation, and half rotation. These triangles with a computed lower bound of  $\gamma(K)$  are displayed in Figure 4. We obtain the improved bound  $5.52 \leq \gamma$ . (For comparison,  $c_{\text{Korn}}^{-2}(\pi^{-2} + c_{\text{tr}})^{-1} = 0.032098$ .) Since  $\|v\|_{L^2(K)}^2 \leq \gamma(K)^{-1} h_K^2 \|\varepsilon(v)\|_{L^2(K)}^2$  for any  $v \in V(K)$ ,  $\beta = \gamma^{-1} h_{\max}^2$  in (C). The choice  $\sigma = 2.76$  in Corollary 5.5 leads to the LEB

$$\text{LEB}(j) = \min\{1, 1/(1/2 + h_{\max}^2 \lambda_h(j)/5.52)\} \lambda_h(j) \leq \lambda(j)$$

for the linear elasticity eigenvalue problem. Figure 5 displays the convergence history plot of  $\lambda_C(1) - \text{LEB}(1)$  with improved accuracy in comparison to Figure 3.

**6.5. Conclusions.** In all examples, adaptive computation recovers optimal convergence rates of the lower eigenvalue bounds towards the exact eigenvalue. Accurate upper bounds of constants in local compact embeddings can be computed and improve the quality of the lower eigenvalue bounds. Additional applications beyond those presented in this paper include general scalar elliptic operators (instead of Laplace) and the biharmonic eigenvalue problem in 2d, where the property (1.7) is possible [17]. The 3d case remains open. Another application is the Stokes eigenvalue problem in primal form, where the vanishing divergence is enforced by using the reconstruction  $\text{div}_h$  from Remark 5.7 on the discrete level. Since the conditions (B)–(C) arise from local estimates in practice, the analysis extends to piecewise constant  $\sigma$  for improved handling of variable material parameters, e.g., in linear elasticity.

## REFERENCES

- [1] M. Bebendorf. A note on the Poincaré inequality for convex domains. In: *Z. Anal. Anwendungen* 22.4 (2003), 751–756.
- [2] F. Bertrand, C. Carstensen, B. Gräßle and N. T. Tran. Stabilization-free HHO a posteriori error control. In: *Numer. Math.* 154.3–4 (2023), 369–408.
- [3] S. C. Brenner. Korn's inequalities for piecewise  $H^1$  vector fields. In: *Math. Comp.* 73.247 (2004), 1067–1087.
- [4] C. Carstensen, A. Ern and S. Puttkammer. Guaranteed lower bounds on eigenvalues of elliptic operators with a hybrid high-order method. In: *Numer. Math.* 149.2 (2021), 273–304.
- [5] C. Carstensen and D. Gallistl. Guaranteed lower eigenvalue bounds for the biharmonic equation. In: *Numer. Math.* 126.1 (2014), 33–51.
- [6] C. Carstensen and J. Gedicke. Guaranteed lower bounds for eigenvalues. In: *Math. Comp.* 83.290 (2014), 2605–2629.
- [7] C. Carstensen, B. Gräßle and N. T. Tran. Adaptive hybrid high-order method for guaranteed lower eigenvalue bounds. In: *Numer. Math.* 156.3 (2024), 813–851.
- [8] C. Carstensen and S. Puttkammer. Adaptive guaranteed lower eigenvalue bounds with optimal convergence rates. In: *Numer. Math.* 156.1 (2024), 1–38.
- [9] C. Carstensen and S. Puttkammer. Direct guaranteed lower eigenvalue bounds with optimal a priori convergence rates for the bi-Laplacian. In: *SIAM J. Numer. Anal.* 61.2 (2023), 812–836.
- [10] C. Carstensen and N. T. Tran. Locking-free hybrid high-order method for linear elasticity. In: *arXiv:2404.02768* (2024).
- [11] C. Carstensen, Q. Zhai and R. Zhang. A skeletal finite element method can compute lower eigenvalue bounds. In: *SIAM J. Numer. Anal.* 58.1 (2020), 109–124.
- [12] M. Costabel and M. Dauge. On the inequalities of Babuška-Aziz, Friedrichs and Horgan-Payne. In: *Arch. Ration. Mech. Anal.* 217.3 (2015), 873–898.
- [13] D. A. Di Pietro and J. Droniou. The hybrid high-order method for polytopal meshes. Vol. 19. MS&A. Modeling, Simulation and Applications. Design, analysis, and applications. Springer, Cham, 2020, xxxi+525.

- [14] D. A. Di Pietro and A. Ern. Mathematical aspects of discontinuous Galerkin methods. Vol. 69. *Mathématiques & Applications*. Springer, Heidelberg, 2012, xviii+384.
- [15] D. A. Di Pietro and A. Ern. A hybrid high-order locking-free method for linear elasticity on general meshes. In: *Comput. Methods Appl. Mech. Engrg.* 283 (2015), 1–21.
- [16] D. A. Di Pietro, A. Ern and S. Lemaire. An arbitrary-order and compact-stencil discretization of diffusion on general meshes based on local reconstruction operators. In: *Comput. Methods Appl. Math.* 14.4 (2014), 461–472.
- [17] Z. Dong and A. Ern. Hybrid high-order and weak Galerkin methods for the biharmonic problem. In: *SIAM J. Numer. Anal.* 60.5 (2022), 2626–2656.
- [18] A. Ern and P. Zanotti. A quasi-optimal variant of the hybrid high-order method for elliptic partial differential equations with  $H^{-1}$  loads. In: *IMA J. Numer. Anal.* 40.4 (2020), 2163–2188.
- [19] D. Gallistl. Adaptive nonconforming finite element approximation of eigenvalue clusters. In: *Comput. Methods Appl. Math.* 14.4 (2014), 509–535.
- [20] D. Gallistl. Mixed methods and lower eigenvalue bounds. In: *Math. Comp.* 92.342 (2023), 1491–1509.
- [21] D. Gallistl and V. Olkhovskiy. Computational lower bounds of the Maxwell eigenvalues. In: *SIAM J. Numer. Anal.* 61.2 (2023), 539–561.
- [22] X. Liu and S. Oishi. Verified eigenvalue evaluation for the Laplacian over polygonal domains of arbitrary shape. In: *SIAM J. Numer. Anal.* 51.3 (2013), 1634–1654.
- [23] G. Strang and G. J. Fix. An analysis of the finite element method. Prentice-Hall Series in Automatic Computation. Prentice-Hall, Inc., Englewood Cliffs, NJ, 1973, xiv+306.
- [24] C. You, H. Xie and X. Liu. Guaranteed eigenvalue bounds for the Steklov eigenvalue problem. In: *SIAM J. Numer. Anal.* 57.3 (2019), 1395–1410.

(N. T. Tran) INSTITUT FÜR MATHEMATIK, UNIVERSITÄT AUGSBURG, 86159 AUGSBURG, GERMANY

*Email address:* `ngoc.tien.tran@uni-a.de`